Soft nuclear equations of state for super-massive neutron star

K. Miyazaki

E-mail: miyazakiro@rio.odn.ne.jp

Abstract

Two new nuclear equations of state (EOSs) are proposed and are applied to neutron star (NS). They predict the incompressibilities $K_0 = 179$MeV and 230MeV, respectively. The density dependencies of nuclear symmetry energies are consistent with the recent analyses of heavy-ion reactions. We can reproduce the recently observed super-massive NS of $M_G > 2.5M_\odot$, the mass-radius relation of EXO 0748-676 and the large radius $R > 13$km of RX J1856.5-3754. No direct URCA in NS is consistent with the standard scenario of NS cooling. Because most of modern EOSs of NS matter cannot satisfy all these constraints, our EOSs are excellent.

Nuclear equation of state (EOS) is a long-standing subject in nuclear physics. Recently, we have new insights into its isovector part from the progress in terrestrial experiments of heavy-ion reactions and astronomical observations of neutron stars (NSs). Especially, information [1-8] on the density dependence of nuclear symmetry energy is important. It plays a significant role [9-11] in determining proton fraction in the core of NS and radius of NS. The former is an essential ingredient in the possibility of the direct URCA cooling in NS. According to the standard scenario of NS cooling, the direct URCA process is forbidden and so the proton fraction is severely constrained. Consequently, nuclear symmetry energy is also constrained.

The symmetry energy $E_s(\rho_B)$ can be expanded [8,12] around the nuclear saturation density $\rho_{B0} = 0.16\text{fm}^{-3}$:

$$E_s\left(\rho_B\right) = E_s\left(\rho_{B0}\right) + \frac{L}{3}\left(\frac{\rho_B - \rho_{B0}}{\rho_{B0}}\right) + \frac{K_s}{18}\left(\frac{\rho_B - \rho_{B0}}{\rho_{B0}}\right)^2, \tag{1}$$

where

$$L = 3\,\rho_{B0}\left.\frac{\partial E_s\left(\rho_B\right)}{\partial \rho_B}\right|_{\rho_B=\rho_{B0}}, \tag{2}$$

$$K_s = 9\,\rho_{B0}^2\left.\frac{\partial^2 E_s\left(\rho_B\right)}{\partial \rho_B^2}\right|_{\rho_B=\rho_{B0}}. \tag{3}$$

L and $K_{asy} \equiv K_s - 6L$ determine the behavior of symmetry energy at high densities. In the analyses of experimental data from heavy-ion collisions [2,8,12,13] they are limited to

the ranges, $L = 88 \pm 25$MeV and $K_{asy} = -500 \pm 50$MeV, respectively. The recent work [14] has shown that these conditions severely select the relativistic mean-field (RMF) models of dense nuclear matter. Only 3 models among all the 23 models are allowed.

Unfortunately, Ref. [14] does not refer to the model developed in Ref. [15]. The first motivation for the present work is to show the excellence of the model and to supplement Ref. [14]. We have introduced in Ref. [15] the renormalized meson-nucleon coupling constants:

$$g^*_{pp\sigma(\omega)} = h_{0p}\, g_{NN\sigma(\omega)} = \frac{1}{2}\left[(1+\lambda_0) + (1-\lambda_0)\left(\left(m^*_p\right)^2 - v_p^2\right)\right] g_{NN\sigma(\omega)}, \tag{4}$$

$$g^*_{nn\sigma(\omega)} = h_{0n}\, g_{NN\sigma(\omega)} = \frac{1}{2}\left[(1+\lambda_0) + (1-\lambda_0)\left(\left(m^*_n\right)^2 - v_n^2\right)\right] g_{NN\sigma(\omega)}, \tag{5}$$

$$g^*_{pp\delta(\rho)} = h_{1p}\, g_{NN\delta(\rho)} = \frac{1}{2}\left[(1+\lambda_1) + (1-\lambda_1)\left(\left(m^*_p\right)^2 - v_p^2\right)\right] g_{NN\delta(\rho)}, \tag{6}$$

$$g^*_{nn\delta(\rho)} = h_{1n}\, g_{NN\delta(\rho)} = \frac{1}{2}\left[(1+\lambda_1) + (1-\lambda_1)\left(\left(m^*_n\right)^2 - v_n^2\right)\right] g_{NN\delta(\rho)}, \tag{7}$$

where $0 \leq \lambda_{0(1)} \leq 1$ are phenomenological parameters. $M^*_{p(n)} = m^*_{p(n)} M_N$ are the effective masses [16] of proton (p) and neutron (n) in asymmetric nuclear matter. $V_{p(n)} = v_{p(n)} M_N$ are their vector potentials. The density dependence of symmetry energy is mostly determined by the isovector renormalization parameter λ_1. A value $\lambda_1 = 0$ reproduces L and K_{asy} that are close to the lowest and highest limits in their allowed ranges. As λ_1 increases we have a higher L and a lower K_{asy}. Consequently, the proton is more abundant in the core of NS. However, no direct URCA cooling in NS imposes a severe constraint $\lambda_1 \leq 0.2$ and so favors a lower L and a higher K_{asy} in their allowed values. The result is consistent with the analyses in Refs. [5] and [6] whose constraints on L and K_{asy} are stronger than Refs. [2,8,12,13].

On the other hand, the isoscalar part of nuclear EOS is well characterized by the incompressibility K_0 of saturated symmetric nuclear matter. In the model of Ref. [15] it is mostly determined by the isoscalar renormalization parameter λ_0 in Eqs. (4) and (5). In practice, Ref. [15] assumed $\lambda_0 = 2/3$ and predicted a stiff EOS of $K_0 = 320$MeV. The result is compatible with 167MeV$\leq K_0 \leq$ 380MeV derived in Ref. [17]. The observations of large gravitational masses $M_G > 2M_\odot$ [18-21] and radii $R >$ 13km [22-25] of NSs also support a stiff EOS. To the contrary, the recent analyses [26-29] of heavy-ion experiments tend to favor the soft EOSs of 170MeV$\leq K_0 \leq$ 230MeV. References [30,31] have attempted to resolve this incompatibility between the terrestrial heavy-ion data and the astronomical observations. They however cannot reproduce the super-massive NS [20,21] of $M_G > 2.5M_\odot$ nor the large radius [23] of RX J1856.5-3754.

The second motivation for the present work is to resolve the above mentioned incompatibility. For the purpose we have to develop a nuclear EOS, which is soft at low density but stiff at high density. As shown above, the incompressibility in Ref. [15] is mostly determined by the isoscalar renormalization parameter λ_0. If we assume $\lambda_0 = 0$, we have

a soft EOS of $K_0 \approx 170$MeV. If we assume $\lambda_0 = 1$, the original Walecka σ-ω model [16] is reproduced. It predicts a significantly stiff EOS of $K_0 \approx 560$MeV. These results suggest that λ_0 should increase from 0 to 1 as the baryon density increases. If λ_0 depends on baryon density, λ_1 should be also dependent on density so that the physically reasonable symmetry energy is reproduced and that the direct URCA cooling of NS is forbidden.

The present paper extends Ref. [15] so that both the isoscalar and isovector renormalization parameters depend on baryon density. However, because the theoretical derivation of their density dependencies is far beyond the RMF model, we assume purely phenomenological density-dependencies in rather intuitive ways. First, we use a following function for λ_0:

$$\lambda_0 = 1 - \frac{1}{1 + \exp\left[\,2\left(\rho_B/\rho_{B0} - d_0\right)\right]}, \tag{8}$$

where a parameter d_0 is adjusted so as to reproduce a given incompressibility. The value of λ_0 increases steeply in a narrow range so that as will be shown later we can reproduce super-massive NS. We have introduced the baryon density as a c-number against the density dependent hadron field (DDHF) theory [32]. It is noted that our renormalized coupling constants $g^*_{NN\sigma(\omega)}$ already depend on baryon density implicitly through the effective mass m^* and the vector potential v even if λ_0 is a constant. Such an implicit density-dependence does not produce the so-called rearrangement contributions as in the DDHF theory. It is therefore hopeful that λ_0 also depends on baryon density implicitly. It is however difficult to find an appropriate function for λ_0 in terms of m^* and v because they are determined self-consistently. To the contrary, an appropriate function in terms of ρ_B/ρ_{B0} can be found intuitively. Consequently, we operate $g^*_{NN\sigma(\omega)}$ as if they were implicitly dependent on the baryon density. We do not take into account the contributions due to $\partial g^*_{NN\sigma(\omega)}/\partial\rho_B$, which lead to the rearrangement terms [32] in vector self-energy. Nevertheless, we believe that the present investigation offers a physically valuable insight into a reasonable EOS of dense nuclear matter.

Because $\partial g^*_{NN\sigma(\omega)}/\partial\rho_B$ is neglected, the saturation property of symmetric nuclear matter is calculated in the same way as Ref. [15]. The effective mass m^*_0 at saturation density is determined by solving the nonlinear equation:

$$\frac{1}{2}\left(\frac{E^*_{F0}}{M_N} - m^*_0\,\frac{\rho_{S0}}{\rho_{B0}}\right) - \frac{AB}{D}\,(1 - m^*_0) + \frac{A\,C}{D}\,v_0 = 0, \tag{9}$$

where

$$A = (1 + \lambda_0) + (1 - \lambda_0)\left[\,(m^*_0)^2 - v_0^2\,\right], \tag{10}$$

$$B = \left[(1 + \lambda_0) + (1 - \lambda_0)\left((m^*_0)^2 + v_0^2\right)\right](\rho_{S0}/\rho_{B0}) + 2\,(1 - \lambda_0)\,m^*_0\,v_0, \tag{11}$$

$$C = (\lambda_0 + 1) + (\lambda_0 - 1)\left[\,(m^*_0)^2 - 2\,m^*_0 + v_0^2\,\right] + 2\,(1 - \lambda_0)\,(1 - m^*)\,v_0\,(\rho_{S0}/\rho_{B0})\,, \tag{12}$$

$$D = \left[(\lambda_0+1)+(\lambda_0-1)\left((m_0^*)^2-2\,m_0^*+v_0^2\right)\right]\left[(1+\lambda_0)+(1-\lambda_0)\left((m_0^*)^2+v_0^2\right)\right] - 4\,(1-\lambda_0)^2\,(1-m_0^*)\,m_0^*\,v_0^2. \quad (13)$$

$E_F^* = \left(k_F^2+(M^*)^2\right)^{1/2}$ and ρ_{S0} are the Fermi energy and the scalar density of symmetric nuclear matter at saturation density ρ_{B0}. The vector potential $V_0 = v_0 M_N$ at saturation density is given by

$$V_0 = M + W_0 - E_{F0}^*. \quad (14)$$

$W_0 = -15.75$MeV is the saturation energy. It is noted again that a constant value $1-[1+\exp(2\,(1-d_0))]^{-1}$ is assumed for λ_0. We can see that Eq. (14) is independent on a model. This is the result of Hugenholtz-van Hove theorem. If $\partial g^*_{NN\sigma(\omega)}/\partial\rho_B$ is taken into account, the theorem is broken unless the rearrangement contributions are included. The $NN\sigma$ and $NN\omega$ coupling constants are determined by

$$\frac{g_{NN\sigma}^2}{m_\sigma^2} = \frac{4\,D}{A^3 B}\,\frac{(1-m_0^*)\,M_N}{\rho_{B0}}, \quad (15)$$

$$\frac{g_{NN\omega}^2}{m_\omega^2} = \frac{4\,D}{A^3\,C}\,\frac{V_0}{\rho_{B0}}. \quad (16)$$

In the present work we investigate two models of incompressibility. The first assumes $d_0 = 2.0$ in Eq. (8). The resultant incompressibility $K_0 = 179$MeV agrees with the value derived from the analysis [28] of kaon production at sub-threshold energies in heavy-ion collisions. The second assumes $d_0 = 1.2$ and predicts $K_0 = 230$MeV that agrees with the values derived from the analyses of giant monopole resonance [33] and heavy-ion fusion reaction [34]. Table 1 summarizes the $NN\sigma$ and $NN\omega$ coupling constants, the effective mass m_0^*, the vector potential V_0 and the incompressibility K_0 at saturation density. The coupling constants are different from those in the Bonn potential [35]. The discrepancies are common to all the RMF models. It is however noted that our results are closer to Bonn potential than the other RMF models. The values of effective mass are somewhat larger than $m_0^* \simeq 0.6$, which is necessary [36] for the reasonable spin-orbit splitting of finite nuclei but obliges us to a rather stiff EOS of $K_0 = 320$MeV. This is because the effective mass is relatively insensitive to a value of λ_0 while the incompressibility is rather sensitive to it.

Next, the model is applied to asymmetric nuclear matter. As the isoscalar coupling constants we assume a purely phenomenological density dependence of the isovector renormalization parameter λ_1 in Eqs. (6) and (7):

$$\lambda_1 = 1 - \frac{1}{1+\exp\left(\rho_B/\rho_{B0}-4\right)}. \quad (17)$$

This is because the symmetry energy favors $\lambda_1 \ll 1$ at saturation density and because λ_1

should increases much more slowly than λ_0 so that the fraction of neutron in the core of NS is enough for no direct URCA cooling of NS. The contributions due to $\partial g^*_{NN\delta(\rho)}/\partial\rho_B$ are also neglected. Therefore, asymmetric nuclear matter is also calculated in the same way as Ref. [15]. The effective masses $M^*_{p(n)} = m^*_{p(n)}M$ and the vector potentials $V_{p(n)} = v_{p(n)}M$ are determined by solving 4th rank nonlinear simultaneous equations:

$$\rho_{Bp(n)} + m_\sigma^2 \frac{\langle\sigma\rangle}{M}\frac{\partial\langle\sigma\rangle}{\partial v_{p(n)}} + m_\delta^2 \frac{\langle\delta_3\rangle}{M}\frac{\partial\langle\delta_3\rangle}{\partial v_{p(n)}} - m_\omega^2 \frac{\langle\omega_0\rangle}{M}\frac{\partial\langle\omega_0\rangle}{\partial v_{p(n)}} - m_\rho^2 \frac{\langle\rho_{03}\rangle}{M}\frac{\partial\langle\rho_{03}\rangle}{\partial v_{p(n)}} = 0, \quad (18)$$

$$\rho_{Sp(n)} + m_\sigma^2 \frac{\langle\sigma\rangle}{M}\frac{\partial\langle\sigma\rangle}{\partial m^*_{p(n)}} + m_\delta^2 \frac{\langle\delta_3\rangle}{M}\frac{\partial\langle\delta_3\rangle}{\partial m^*_{p(n)}} - m_\omega^2 \frac{\langle\omega_0\rangle}{M}\frac{\partial\langle\omega_0\rangle}{\partial m^*_{p(n)}} - m_\rho^2 \frac{\langle\rho_{03}\rangle}{M}\frac{\partial\langle\rho_{03}\rangle}{\partial m^*_{p(n)}} = 0. \quad (19)$$

The mean-fields are expressed in terms of the effective masses and the vector potentials:

$$\langle\sigma\rangle = \frac{M}{g_{NN\sigma}}\frac{h_{1n}\left(1-m_p^*\right) + h_{1p}\left(1-m_n^*\right)}{H}, \quad (20)$$

$$\langle\delta_3\rangle = \frac{M}{g_{NN\delta}}\frac{h_{0n}\left(1-m_p^*\right) - h_{0p}\left(1-m_n^*\right)}{H}, \quad (21)$$

$$\langle\omega_0\rangle = \frac{M}{g_{NN\omega}}\frac{h_{1n}v_p + h_{1p}v_n}{H}, \quad (22)$$

$$\langle\rho_{03}\rangle = \frac{M}{g_{NN\rho}}\frac{h_{0n}v_p - h_{0p}v_n}{H}, \quad (23)$$

where

$$H = h_{0p}h_{1n} + h_{0n}h_{1p}. \quad (24)$$

The derivatives of mean-fields are

$$H\frac{\partial\langle\sigma\rangle}{\partial v_p} = \left\{\left[\left(1-\lambda_1\right)h_{0n} + \left(1-\lambda_0\right)h_{1n}\right]\langle\sigma\rangle - \left(1-\lambda_1\right)\frac{\left(1-m_n^*\right)M}{g_{NN\sigma}}\right\}v_p, \quad (25)$$

$$H\frac{\partial\langle\delta_3\rangle}{\partial v_p} = \left\{\left[\left(1-\lambda_1\right)h_{0n} + \left(1-\lambda_0\right)h_{1n}\right]\langle\delta_3\rangle + \left(1-\lambda_0\right)\frac{\left(1-m_n^*\right)M}{g_{NN\delta}}\right\}v_p, \quad (26)$$

$$H\frac{\partial\langle\omega_0\rangle}{\partial v_p} = \left\{\left[\left(1-\lambda_1\right)h_{0n} + \left(1-\lambda_0\right)h_{1n}\right]\langle\omega_0\rangle - \left(1-\lambda_1\right)\frac{v_nM}{g_{NN\omega}}\right\}v_p + \frac{M}{g_{NN\omega}}h_{1n}, \quad (27)$$

$$H\frac{\partial\langle\rho_{03}\rangle}{\partial v_p} = \left\{\left[\left(1-\lambda_1\right)h_{0n} + \left(1-\lambda_0\right)h_{1n}\right]\langle\rho_{03}\rangle + \left(1-\lambda_0\right)\frac{v_nM}{g_{NN\rho}}\right\}v_p + \frac{M}{g_{NN\rho}}h_{0n}, \quad (28)$$

$$H\frac{\partial\langle\sigma\rangle}{\partial v_n} = \left\{\left[\left(1-\lambda_1\right)h_{0p} + \left(1-\lambda_0\right)h_{1p}\right]\langle\sigma\rangle - \left(1-\lambda_1\right)\frac{\left(1-m_p^*\right)M}{g_{NN\sigma}}\right\}v_n, \quad (29)$$

$$H\frac{\partial\langle\delta_3\rangle}{\partial v_n} = \left\{\left[\left(1-\lambda_1\right)h_{0p} + \left(1-\lambda_0\right)h_{1p}\right]\langle\delta_3\rangle - \left(1-\lambda_0\right)\frac{\left(1-m_p^*\right)M}{g_{NN\delta}}\right\}v_n, \quad (30)$$

$$H\frac{\partial\langle\omega_0\rangle}{\partial v_n}=\left\{\left[(1-\lambda_1)h_{0p}+(1-\lambda_0)h_{1p}\right]\langle\omega_0\rangle-(1-\lambda_1)\frac{v_pM}{g_{NN\omega}}\right\}v_n+\frac{M}{g_{NN\omega}}h_{1p}, \quad (31)$$

$$H\frac{\partial\langle\rho_{03}\rangle}{\partial v_n}=\left\{\left[(1-\lambda_1)h_{0p}+(1-\lambda_0)h_{1p}\right]\langle\rho_{03}\rangle-(1-\lambda_0)\frac{v_pM}{g_{NN\rho}}\right\}v_n-\frac{M}{g_{NN\rho}}h_{0p}, \quad (32)$$

$$H\frac{\partial\langle\sigma\rangle}{\partial m_p^*}=\left\{(1-\lambda_1)\frac{(1-m_n^*)M}{g_{NN\sigma}}-\left[(1-\lambda_1)h_{0n}+(1-\lambda_0)h_{1n}\right]\langle\sigma\rangle\right\}m_p^*-\frac{M}{g_{NN\sigma}}h_{1n}, \quad (33)$$

$$H\frac{\partial\langle\delta_3\rangle}{\partial m_p^*}=-\left\{(1-\lambda_0)\frac{(1-m_n^*)M}{g_{NN\delta}}+\left[(1-\lambda_1)h_{0n}+(1-\lambda_0)h_{1n}\right]\langle\delta_3\rangle\right\}m_p^*-\frac{M}{g_{NN\delta}}h_{0n}, \quad (34)$$

$$H\frac{\partial\langle\omega_0\rangle}{\partial m_p^*}=\left\{(1-\lambda_1)\frac{v_nM}{g_{NN\omega}}-\left[(1-\lambda_1)h_{0n}+(1-\lambda_0)h_{1n}\right]\langle\omega_0\rangle\right\}m_p^*, \quad (35)$$

$$H\frac{\partial\langle\rho_{03}\rangle}{\partial m_p^*}=-\left\{(1-\lambda_0)\frac{v_nM}{g_{NN\rho}}+\left[(1-\lambda_1)h_{0n}+(1-\lambda_0)h_{1n}\right]\langle\rho_{03}\rangle\right\}m_p^*, \quad (36)$$

$$H\frac{\partial\langle\sigma\rangle}{\partial m_n^*}=\left\{(1-\lambda_1)\frac{\left(1-m_p^*\right)M}{g_{NN\sigma}}-\left[(1-\lambda_1)h_{0p}+(1-\lambda_0)h_{1p}\right]\langle\sigma\rangle\right\}m_n^*-\frac{M}{g_{NN\sigma}}h_{1p}, \quad (37)$$

$$H\frac{\partial\langle\delta_3\rangle}{\partial m_n^*}=\left\{(1-\lambda_0)\frac{\left(1-m_p^*\right)M}{g_{NN\delta}}-\left[(1-\lambda_1)h_{0p}+(1-\lambda_0)h_{1p}\right]\langle\delta_3\rangle\right\}m_n^*+\frac{M}{g_{NN\delta}}h_{0p}, \quad (38)$$

$$H\frac{\partial\langle\omega_0\rangle}{\partial m_n^*}=\left\{(1-\lambda_1)\frac{v_pM}{g_{NN\omega}}-\left[(1-\lambda_1)h_{0p}+(1-\lambda_0)h_{1p}\right]\langle\omega_0\rangle\right\}m_n^*, \quad (39)$$

$$H\frac{\partial\langle\rho_{03}\rangle}{\partial m_n^*}=\left\{(1-\lambda_0)\frac{v_pM}{g_{NN\rho}}-\left[(1-\lambda_1)h_{0p}+(1-\lambda_0)h_{1p}\right]\langle\rho_{03}\rangle\right\}m_n^*. \quad (40)$$

We still have to specify the isovector-meson coupling constants. For δ-meson coupling constant we use the same value as Bonn A potential in Ref. [35]. The ρ-meson coupling constant is determined so as to reproduce nuclear symmetry energy $E_s(\rho_{B0})=31.6$MeV [1,2] at saturation density. The resultant $g_{NN\rho}$ and the density-dependence of symmetry energy in Eqs. (1-3) are also listed in Table 1. We have to note again that they are calculated for a constant value $1-\left[1+\exp\left(-3\right)\right]^{-1}$ of λ_1. The value of $g_{NN\rho}$ is much larger than Bonn A potential. The disagreement is common to all the RMF models. Both the values of L and K_{asy} are well within the experimental constraints [2,8,12,13] $L=88\pm25$MeV and $K_{asy}=-500\pm50$MeV. As expected from the small λ_1, L is close to the lowest limit.

Then, we develop the EOS of cold neutrino-free non-rotating NS matter. For the purpose we have to add the contributions of electron and muon. They are treated as the free relativistic Fermi gases but couple to baryons through the chemical equilibrium condition

$$\mu_n-\mu_p=\mu_{e^-}=\mu_{\mu^-}, \quad (41)$$

and the charge neutral condition

$$\rho_{Bp} = \rho_{e^-} + \rho_{\mu^-}. \tag{42}$$

The baryon chemical potential is defined by

$$\mu_{p(n)} = E^*_{Fp(n)} + V_{p(n)}, \tag{43}$$

where $E^*_{Fp(n)} = \left(k^2_{Fp(n)} + {M^*_{p(n)}}^2\right)^{1/2}$ is the Fermi energy of proton (neutron). We solve 6th rank nonlinear simultaneous equations (18), (19), (42) and the baryon number conservation:

$$\rho_B = \rho_{Bp} + \rho_{Bn}. \tag{44}$$

Consequently, $m^*_{p(n)}$, $v_{p(n)}$, μ_n and μ_{e^-} are determined at a given baryon density ρ_B. The energy density of NS matter is calculated by

$$\begin{aligned}\mathcal{E} &= \sum_{i=p,n}\left[\frac{1}{4}\left(3E^*_{Fi}\,\rho_{Bi} + M^*_i\,\rho_{Si}\right) + V_i\,\rho_{Bi}\right] + \frac{1}{4}\sum_{l=e,\mu^-}\left(3E_{Fl}\,\rho_l + m_l\,\rho_{Sl}\right) \\ &+ \frac{1}{2}\,m^2_\sigma\,\langle\sigma\rangle^2 - \frac{1}{2}\,m^2_\omega\,\langle\omega_0\rangle^2 + \frac{1}{2}\,m^2_\delta\,\langle\delta_3\rangle^2 - \frac{1}{2}\,m^2_\rho\,\langle\rho_{03}\rangle^2.\end{aligned} \tag{45}$$

The pressure of NS matter is calculated in terms of the Gibbs-Duhem relation $P = \mu_n\rho_B - \mathcal{E}$.

The resultant EOSs of NS matter on the incompressibilities $K_0 = 179$MeV and 230MeV are tabulated in Table 2. Using the EOSs the mass and the radius of NS are calculated by integrating Tolman-Oppenheimer-Volkov equation [37]:

$$\frac{d\,M_G\,(r)}{d\,r} = \frac{4\,\pi^2}{c^2}\,r^2\,\mathcal{E}\,(r)\,, \tag{46}$$

$$\frac{d\,P\,(r)}{d\,r} = -\frac{G}{c^2}\,\frac{\left[\,\mathcal{E}(r) + P\,(r)\,\right]\left[\,M_G\,(r) + 4\,\pi\,r^3 P\,(r)/c^2\,\right]}{r\left[\,r - 2\,GM_G\,(r)/c^2\,\right]}, \tag{47}$$

where $P\,(r)$, $\mathcal{E}\,(r)$ and $M_G\,(r)$ are the radial distributions of pressure, energy and gravitational mass of NS. For the crust of NS at low densities, we use the EOSs by Feynman-Metropolis-Teller, Baym-Pethick-Sutherland and Negele-Vautherin from Ref. [38]. Our EOSs of NS core cross over the EOS of Negele-Vautherin near $\rho_B = 0.06\text{fm}^{-3}$ and 0.04fm^{-3}, respectively.

Figures 1 and 2 show the gravitational masses of NSs as functions of their radius and central baryon density, respectively. The dashed and solid black curves are calculated using the EOSs of $K_0 = 179$MeV and 230MeV. The gravitational masses of the most massive NSs are $M_G = 2.581M_\odot$ and $2.817M_\odot$, respectively. Their radii are $R = 11.8$km and 12.9km, respectively. Their central baryon densities are $\rho_B = 0.736\text{fm}^{-3}$ and 0.649fm^{-3},

respectively. The result exhibits an excellent success of our model because most of modern EOSs [39-42] cannot reproduce the recently observed [20,21] super-massive NS of $M_G > 2.5M_\odot$.

The red line in Fig. 1 is the mass-radius relation of EXO 0748-676 [43,44], which causes the controversies [45-47] about a possibility of quark matter in NS core. It excludes the most widely referred EOS in Ref. [48]. It also excludes the EOS from the RMF model in Ref. [49], which predicts the same incompressibility $K_0 = 230$MeV as one of our models, while our EOS is successful irrespective of the incompressibility. (In fact, the model in Ref. [49] cannot reproduce the experimental values of L and K_{asy} and so has been already ruled out in Ref. [14].) On the other hand, there are some observations [22,23,25] that strongly suggest the large radius of the isolated NS RX J1856.3754. The blue curve in Fig. 1 is the observed mass-radius relation in Ref. [23]. If RX J1856.3754 is a typical NS of $M_G < 1.5M_\odot$, the rather soft EOS of $K_0 = 179$MeV is excluded. Consequently, the sub-threshold kaon production [20] must be re-investigated.

The black curves in Fig. 3 show proton fractions in the core of NS. The red curve is a value

$$f_p^{DU} = \frac{1}{1 + \left(1 + k_{Fe}/k_{Fp}\right)^3}, \tag{48}$$

where k_{Fe} and k_{Fp} are the Fermi momenta of electron and proton. If the fraction exceeds f_p^{DU}, the direct URCA cooling is allowed in NSs. That occurs above $\rho_B = 0.69\text{fm}^{-3}$ and 0.73fm^{-3}, respectively. On the other hand, the black dashed and solid curves in Fig. 2 exceed $M_G = 1.5M_\odot$ indicated by the red lines above $\rho_B = 0.317\text{fm}^{-3}$ and 0.401fm^{-3}, respectively. Consequently, our EOSs are consistent with the standard scenario of NS cooling [39] in which the direct URCA process is forbidden in typical NSs of $M_G < 1.5M_\odot$. Moreover, as seen from the central baryon densities of the most massive NSs in Fig. 2, for the EOS of $K_0 = 179$MeV the direct URCA cooling is possible only in the super-massive NSs of $M_G > 2.5M_\odot$ while for the EOS of $K_0 = 230$MeV there is no possibility of direct URCA cooling in NSs. The results exhibit an excellent feature of our EOSs because some modern EOSs [39,50] allow the direct URCA cooling even in typical NSs.

Finally, we note that the fundamental microscopic theories as in Refs. [48] and [50] are not necessarily successful. This is because the nucleon-nucleon interaction in highly asymmetric dense nuclear matter is essentially different from the interaction in free space. At present we have no confirm information on it. We should rather deduce it from the phenomenological analyses of heavy-ion collisions and NS observations. The present investigation taking into account the renormalized coupling constants is therefore meaningful.

We have extended the RMF model in Ref. [15] so that the parameters in the renormalized meson-nucleon coupling constants vary with baryon density. However, we do not take into account their derivatives with respect to density. The two phenomenological functions are assumed for the isoscalar renormalization parameter. They reproduce a

rather soft EOS of symmetric nuclear matter with incompressibility $K_0 = 179$MeV and a relatively soft EOS with $K_0 = 230$MeV. On the other hand, a common function is assumed for the isovector renormalization parameter. The resultant symmetry energies of asymmetric nuclear matter show reasonable density dependencies to be consistent with the recent analyses of heavy-ion collisions.

Then, we develop EOSs of NS matter and solve Tolman-Oppenheimer-Volkov equation. We can reproduce the recently observed super-massive NS of $M_G > 2.5M_\odot$. The mass-radius relation of EXO 0748-676 is satisfied. Especially, the relatively soft EOS of $K_0 = 230$MeV can reproduce the large radius $R > 13$km of RX J1856.5-3754. Moreover, the direct URCA cooling of NS is forbidden in consistence with the standard scenario. Because most of modern EOSs of NS matter cannot satisfy all the above constraints, our EOSs are excellent.

However, the precise observations of mass and radius of NSs are difficult. In fact, the recent calculation [51] of mergers of binary NSs suggests that the maximum NS mass must be within $2.0M_\odot < M_G < 2.5M_\odot$. There are still questions [52,53] about the observations of EXO 0748-676 in Refs. [43,44]. There are analyses [54,55] asserting that the radius of RX J1856.5-3754 is much shorter than the value in Ref. [23]. RX J1856.5-3754 might be a strange star [56-58] rather than a normal NS. The recent observation [59] of X-ray pulsar SAX J1808.4-3658 also indicates a short radius $R < 12$km and so obviously contradicts our EOSs of NS matter. Moreover, Ref. [60] suggests that the direct URCA process is necessary in SAX J1808.4-3658 against the standard scenario of NS cooling. The other works [61,62] also pointed out possible direct URCA cooling in the cores of massive NSs. In spite of these uncertainties and the purely phenomenological density dependencies in our model, we expect that the EOSs in the present work will be useful references for future investigations because of their unique and excellent characters.

References

[1] L-W. Chen, C.M. Ko and B-A. Li, Phys. Rev. Lett. **94** (2005) 032701 [arXiv:nucl-th/0407032].

[2] B-A. Li and L-W. Chen, Phys. Rev. C **72** (2005) 064611 [arXiv:nucl-th/0508024].

[3] B-A. Li, L-W. Chen, C.M. Ko and A.W. Steiner, arXiv:nucl-th/0601028.

[4] Z-H. Li, L-W. Chen, C.M. Ko, B-A. Li and H-R. Ma, Phys. Rev. C **74** (2006) 044613 [arXiv:nucl-th/0606063].

[5] P. Danielewicz, arXiv:nucl-th/0607030.

[6] D.V. Shetty, S.J. Yennello and G.A. Souliotis, arXiv:nucl-ex/0610019.

[7] G-C. Yong, B-A. Li and L-W. Chen, Phys. Lett. B **650** (2007) 344 [arXiv:nucl-th/0703042].

[8] L-W. Chen, C.M. Ko, B-A. Li and G-C. Yong, Front. Phys. China **2** (2007) 327 [arXiv:nucl-th/0704.2340].

[9] B-A. Li and A.W. Steiner, Phys. Lett. B **642** (2006) 436 [arXiv:nucl-th/0511064].

[10] A.W. Steiner, Phys. Rev. C **74** (2006) 045808 [arXiv:nucl-th/0607040].

[11] B-A. Li, L-W. Chen, C.M. Ko, P.G. Krastev, A.W. Steiner and G-C. Yong, J. Phys. G **35** (2008) 014044.

[12] L-W. Chen, C.M. Ko and B-A. Li, arXiv:nucl-th/0610057.

[13] P. Danielewicz and J. Lee, arXiv:nucl-th/0708.2830.

[14] L-W. Chen, C.M. Ko and B-A. Li, Phys. Rev. C **76** (2007) 054316 [arXiv:nucl-th/0709.0900].

[15] K. Miyazaki, Mathematical Physics Preprint Archive (mp_arc) 06-336.

[16] B.D. Serot and J.D. Walecka, *Advances in Nuclear Physics*, Vol. **16** (Plenum, New York, 1986).

[17] P. Danielewicz, R. Lacey and W.G. Lynch, Science **298** (2002) 1592 [arXiv:nucl-th/0208016].

[18] J.S. Clark *et al.*, Astron. Astrophys. **392** (2002) 909.

[19] D. Barret, J-F. Olive and C. Miller, Mon. Not. Roy. Astron. Soc. **361** (2005) 855 [arXiv:astro-ph/0505402].

[20] P.C.C. Freire, S.M. Ransom, S. Bégin, I.H. Stairs, J.W.T. Hessels, L.H. Frey and F. Camilo, arXiv:astro-ph/0711.0925.

[21] P.C.C. Freire, arXiv:astro-ph/0712.0024.

[22] T.M. Braje and R.W. Romani, Astrophys. J. **580** (2002) 1043.

[23] J.E. Trümper, V. Burwitz, F. Haberl and V.E. Zavlin, Nucl. Phys. Proc. Suppl. **132** (2004) 560 [arXiv:astro-ph/0312600].

[24] C.O. Heinke, G.B. Rybicki, R. Narayan and J.E. Grindlay, Astrophys. J. **644** (2006) 1090 [arXiv:astro-ph/0506563].

[25] W.C.G. Ho, Mon. Not. Roy. Astron. Soc. **380** (2007) 71 [arXiv:astro-ph/0705.4543].

[26] A. Andronic, *et al.*, Phys. Lett. B **612** (2005) 173 [arXiv:nucl-ex/0411024].

[27] Ch. Hartnack, H. Oeschler and J. Aichelin, J. Phys. G **32** (2006) 231 [arXiv:nucl-th/0610115].

[28] Ch. Hartnack, H. Oeschler and J. Aichelin, Phys. Rev. Lett. **96** (2006) 012302 [arXiv:nucl-th/0506087].

[29] P. Senger, J. Phys. G **35** (2008) 014050.

[30] C. Fuchs, J. Phys. G **35** (2008) 014049.

[31] I. Sagert, M. Wietoska, J. Schaffner-Bielich and C. Sturm, J. Phys. G **35** (2008) 014053.

[32] F. Hofmann, C.M. Keil and H. Lenske, Phys. Rev. C **64** (2001) 034314 [arXiv:nucl-th/0007050].

[33] D.H. Youngblood, H.L. Clark and Y-W. Lui, Nucl. Phys. A **649** (1999) 49c.

[34] Ş. Mişicu and H. Esbensen, Phys. Rev. Lett. **96** (2006) 112701 [arXiv:nucl-th/0602064].

[35] R. Brockmann and R. Machleidt, Phys. Rev. C **42** (1990) 1965.

[36] W. Koepf, M.M. Sharma and P. Ring, Nucl. Phys. A **533** (1991) 95.

[37] W.D. Arnett and R.L. Bowers, Astrophys. J. Suppl. **33** (1977) 415.

[38] V. Canuto, Ann. Rev. Astr. Ap. **12** (1974) 167; **13** (1975) 335.

[39] T. Klähn et al., Phys. Rev. C **74** (2006) 035802 arXiv:nucl-th/0602038].

[40] K. Miyazaki, Mathematical Physics Preprint Archive (mp_arc) 06-103. Unfortunately, we mistook the calculations in Table 1. The precise values are $L = 72.1$MeV and $K_{asy} = -411$MeV for EZM1, and $L = 89.8$MeV and $K_{asy} = -536$MeV for EZM2. The empirical value 1 of L is also corrected to 88 ± 25MeV. Consequently, the EZM1 passed all the tests in Table 2. The corresponding descriptions in the paper should be corrected. However, the results in figures and our conclusion are not altered.

[41] J. Lattimer and M. Prakash, Phys. Rep. **442** (2007) 109 [arXiv:astro-ph/0612440].

[42] G.F. Burgio, J. Phys. G **35** (2008) 014048.

[43] J. Cottam, F. Paerels and M. Mendez, Nature **420** (2002) 51 [arXiv:astro-ph/0211126].

[44] F. Őzel, Nature **441** (2006) 1115 [arXiv:astro-ph/0605106].

[45] P. Jaikumar, S. Reddy and A.W. Steiner, Mod. Phys. Lett. A **21** (2006) 1965 [arXiv:astro-ph/0608345].

[46] M. Alford, D. Blaschke, A. Drago, T. Klähn, G. Pagliara and J. Schaffner-Bielich, Nature **445** (2007) E7 [arXiv:astro-ph/0606524].

[47] T. Klähn, *et al.*, Phys. Lett. B **654** (2007) 170 [arXiv:nucl-th/0609067].

[48] A. Akmal, V.R. Pandharipande and D.G. Ravenhall, Phys. Rev. C **58** (1998) 1804 [arXiv:nucl-th/9804027].

[49] J. Piekarewicz, arXiv:nucl-th/0709.2699.

[50] P.G. Krastev and F. Sammarruca, Phys. Rev. C **74** (2006) 025808 [arXiv:nucl-th/0601065].

[51] K. Belczynski, R. O'Shaughnessy, V. Kalogera, F. Rasio, R. Taam and T. Bulik, arXiv:astro-ph/0712.1036.

[52] K.J. Pearson *et al.*, Astrophys. J. **648** (2006) 1169 [arXiv:astro-ph/0605634].

[53] J. Cottam, F. Paerels, M. Méndez, L. Boirin, W.H.G. Lewin, E. Kuulkers and J.M. Miller, Astrophys. J. **672** (2008) 504 [arXiv:astro-ph/0709.4062].

[54] J.A. Pons, F.M. Walter, J. Lattimer, M. Prakash, R. Neuhäuser, P. An, Astrophys. J. **564** (2002) 981.

[55] S.M. Ransom, B.M. Gaensler and P.O. Slane, Astropys. J. **570** (2002) L75.

[56] K. Kohri, K. Iida and K. Sato, Prog. Theor. Phys. **109** (2003) 765 [arXiv:astro-ph/0210259].

[57] R. Turolla, S. Zane and J.J. Drake, Astropys. J. **603** (2004) 265.

[58] J.A. Henderson and D. Page, arXiv:astro-ph/0702234.

[59] D.A. Leahy, S.M. Morsink and C. Cadeau, Astrophys. J. **672** (2008) 1119 [arXiv:astro-ph/0703287].

[60] C.O. Heinke, P.G. Jonker, R. Wijnands and R.E. Taam, Astrophys. J. **660** (2007) 1424 [arXiv:astro-ph/0612232].

[61] D.G. Yakovlev, A.D. Kaminker, P. Haensel and O.Y. Gnedin, Astron. Astrophys. **389** (2002) L24

[62] P.G. Jonker, arXiv:astro-ph/0711.2579.

Table 1: The values of the $NN\sigma$, $NN\omega$ and $NN\rho$ coupling constants, the effective mass m_0^*, the vector potential V_0 and the incompressibility K_0 at saturation density. Moreover, L and $K_{asy} \equiv K_s - 6L$ from Eqs. (1)-(3) are presented.

d_0	$\frac{g^2_{NN\sigma}}{4\pi}$	$\frac{g^2_{NN\omega}}{4\pi}$	$\frac{g^2_{NN\rho}}{4\pi}$	m_0^*	V_0 (MeV)	K_0 (MeV)	L (MeV)	K_{asy}(MeV)
1.2	11.14	16.36	2.72	0.641	266	230	66.4	−480
2.0	11.42	16.21	2.60	0.686	227	179	68.4	−489

Table 2: The EOSs, the pressure P and the energy density $\mathcal{E}$ vs. the baryon density ρ_B, for the core region $0.04\text{fm}^{-3} \leq \rho_B \leq 1.0\text{fm}^{-3}$ in NS.

	$K_0 = 179$MeV		$K_0 = 230$MeV	
ρ_B (cm^{-3})	$\mathcal{E}$ (g · cm^{-3})	P (dyn · cm^{-2})	$\mathcal{E}$ (g · cm^{-3})	P (dyn · cm^{-2})
4.00E+37	− − −	− − −	6.734787E+13	2.225089E+32
6.00E+37	1.009836E+14	4.472167E+32	1.011998E+14	5.405557E+32
8.00E+37	1.348791E+14	9.504490E+32	1.351741E+14	1.035417E+33
1.00E+38	1.689323E+14	1.680757E+33	1.692645E+14	1.718798E+33
1.20E+38	2.031524E+14	2.645941E+33	2.034579E+14	2.606784E+33
1.40E+38	2.375404E+14	3.832806E+33	2.377394E+14	3.715143E+33
1.60E+38	2.720850E+14	5.214226E+33	2.720976E+14	5.097355E+33
1.80E+38	3.067726E+14	6.828684E+33	3.065478E+14	6.929814E+33
2.00E+38	3.415913E+14	8.713147E+33	3.411528E+14	9.489519E+33
2.20E+38	3.765337E+14	1.092917E+34	3.760472E+14	1.321258E+34
2.40E+38	4.116052E+14	1.358431E+34	4.114601E+14	1.871644E+34
2.60E+38	4.468383E+14	1.686192E+34	4.477246E+14	2.675006E+34
2.80E+38	4.823145E+14	2.106235E+34	4.852539E+14	3.804438E+34
3.00E+38	5.181951E+14	2.665039E+34	5.244841E+14	5.311742E+34
3.20E+38	5.547562E+14	3.428762E+34	5.658008E+14	7.216446E+34
3.40E+38	5.924137E+14	4.480325E+34	6.094871E+14	9.510368E+34
3.60E+38	6.317158E+14	5.905545E+34	6.557092E+14	1.217111E+35
3.80E+38	6.732813E+14	7.770798E+34	7.045334E+14	1.517409E+35
4.00E+38	7.176939E+14	1.010615E+35	7.559554E+14	1.849877E+35
4.20E+38	7.654009E+14	1.290674E+35	8.099291E+14	2.213026E+35
4.40E+38	8.166619E+14	1.614822E+35	8.663871E+14	2.605840E+35
4.60E+38	8.715572E+14	1.980251E+35	9.252545E+14	3.027587E+35
4.80E+38	9.300291E+14	2.384575E+35	9.864565E+14	3.477569E+35
5.00E+38	9.919310E+14	2.825958E+35	1.049921E+15	3.954841E+35
5.20E+38	1.057068E+15	3.302889E+35	1.115578E+15	4.457897E+35
5.40E+38	1.125228E+15	3.813858E+35	1.183361E+15	4.984377E+35
5.60E+38	1.196195E+15	4.357036E+35	1.253209E+15	5.530865E+35
5.80E+38	1.269767E+15	4.930015E+35	1.325062E+15	6.092906E+35
6.00E+38	1.345755E+15	5.529639E+35	1.398872E+15	6.665367E+35
6.20E+38	1.423997E+15	6.151998E+35	1.474606E+15	7.243177E+35
6.40E+38	1.504354E+15	6.792652E+35	1.552253E+15	7.822322E+35
6.60E+38	1.586718E+15	7.447090E+35	1.631827E+15	8.400760E+35

(continued from the preceding page)

6.80E+38	1.671017E+15	8.111380E+35	1.713367E+15	8.978899E+35
7.00E+38	1.757211E+15	8.782822E+35	1.796933E+15	9.559458E+35
7.20E+38	1.845297E+15	9.460388E+35	1.882596E+15	1.014682E+36
7.40E+38	1.935295E+15	1.014479E+36	1.970433E+15	1.074616E+36
7.60E+38	2.027243E+15	1.083818E+36	2.060511E+15	1.136265E+36
7.80E+38	2.121186E+15	1.154357E+36	2.152885E+15	1.200088E+36
8.00E+38	2.217168E+15	1.226428E+36	2.247593E+15	1.266454E+36
8.20E+38	2.315223E+15	1.300335E+36	2.344653E+15	1.335622E+36
8.40E+38	2.415373E+15	1.376323E+36	2.444064E+15	1.407752E+36
8.60E+38	2.517625E+15	1.454560E+36	2.545809E+15	1.482901E+36
8.80E+38	2.621974E+15	1.535136E+36	2.649857E+15	1.561049E+36
9.00E+38	2.728403E+15	1.618065E+36	2.756167E+15	1.642107E+36
9.20E+38	2.836887E+15	1.703305E+36	2.864692E+15	1.725942E+36
9.40E+38	2.947398E+15	1.790771E+36	2.975383E+15	1.812389E+36
9.60E+38	3.059902E+15	1.880353E+36	3.088189E+15	1.901270E+36
9.80E+38	3.174370E+15	1.971926E+36	3.203064E+15	1.992408E+36
1.00E+39	3.290772E+15	2.065369E+36	3.319966E+15	2.085633E+36

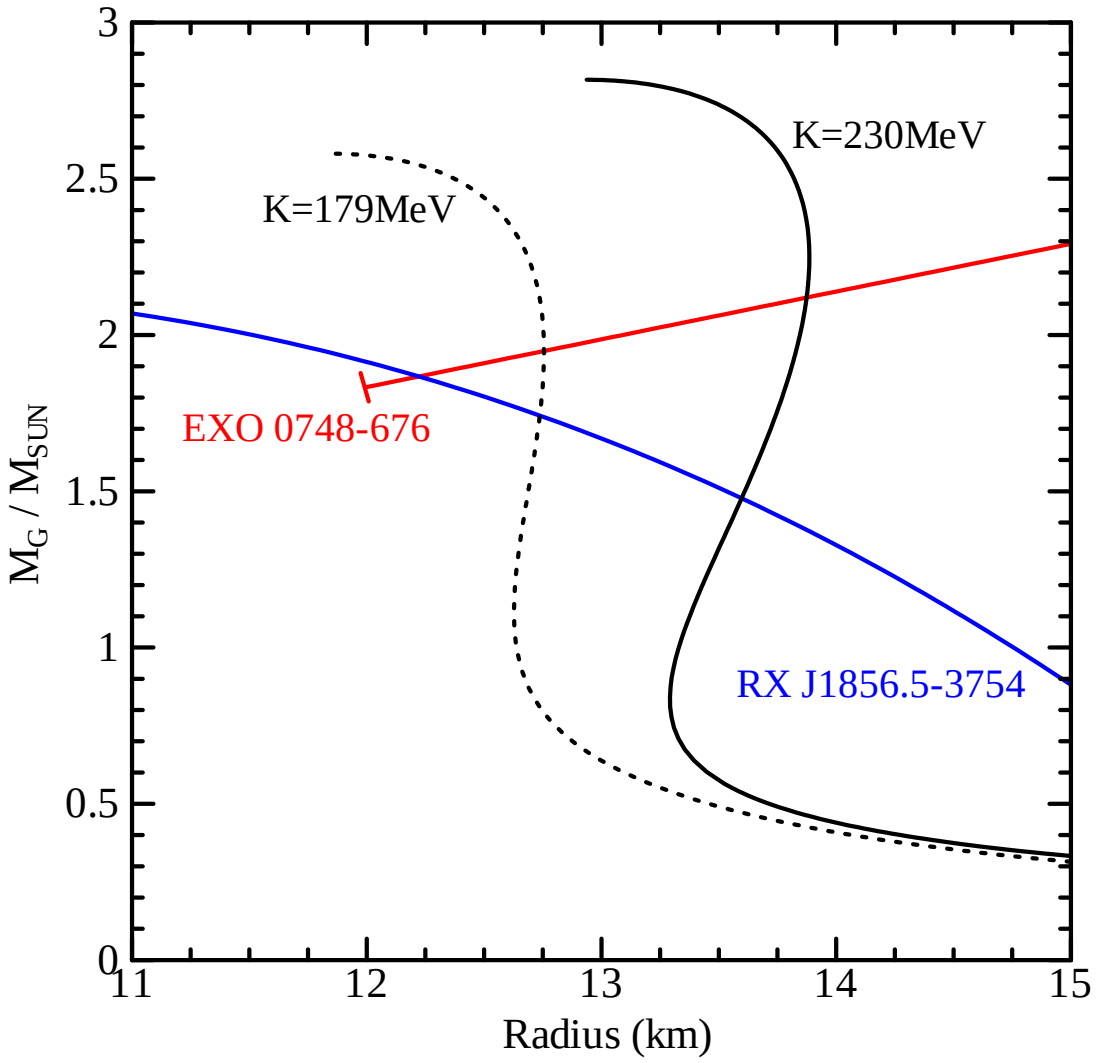

Figure 1: The black dashed and solid curves are the mass-radius relations of NSs using the EOSs of $K_0 = 179$MeV and 230MeV, respectively. The red line and the blue curve are the mass-radius relations of EXO 0748-676 in Ref. [44] and RX J1856.3754 in Ref. [23], respectively.

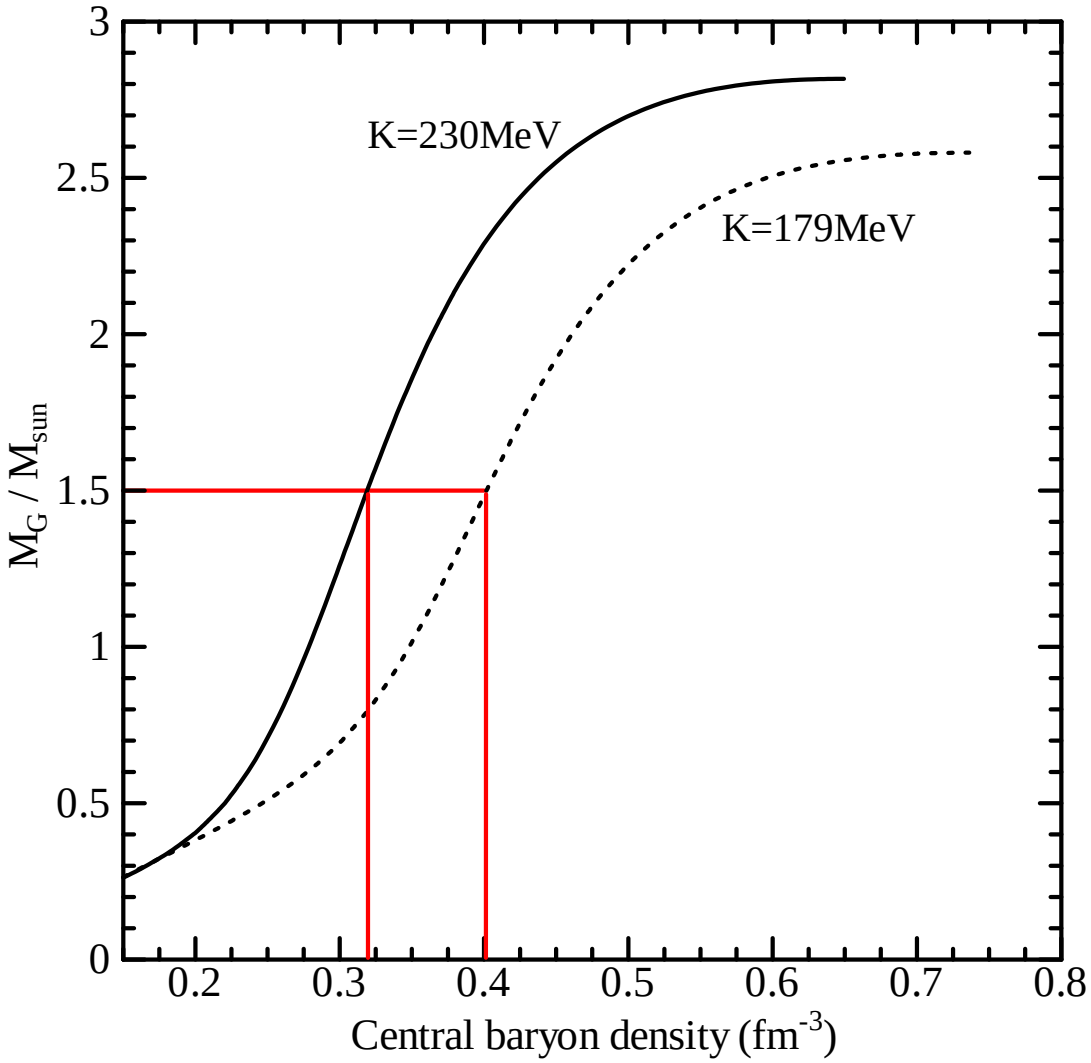

Figure 2: The black dashed and solid curves are the gravitational masses of NSs as functions of their central baryon density using the EOSs of $K_0 = 179$MeV and 230MeV, respectively. The red lines indicate the densities for $M_G = 1.5M_\odot$.

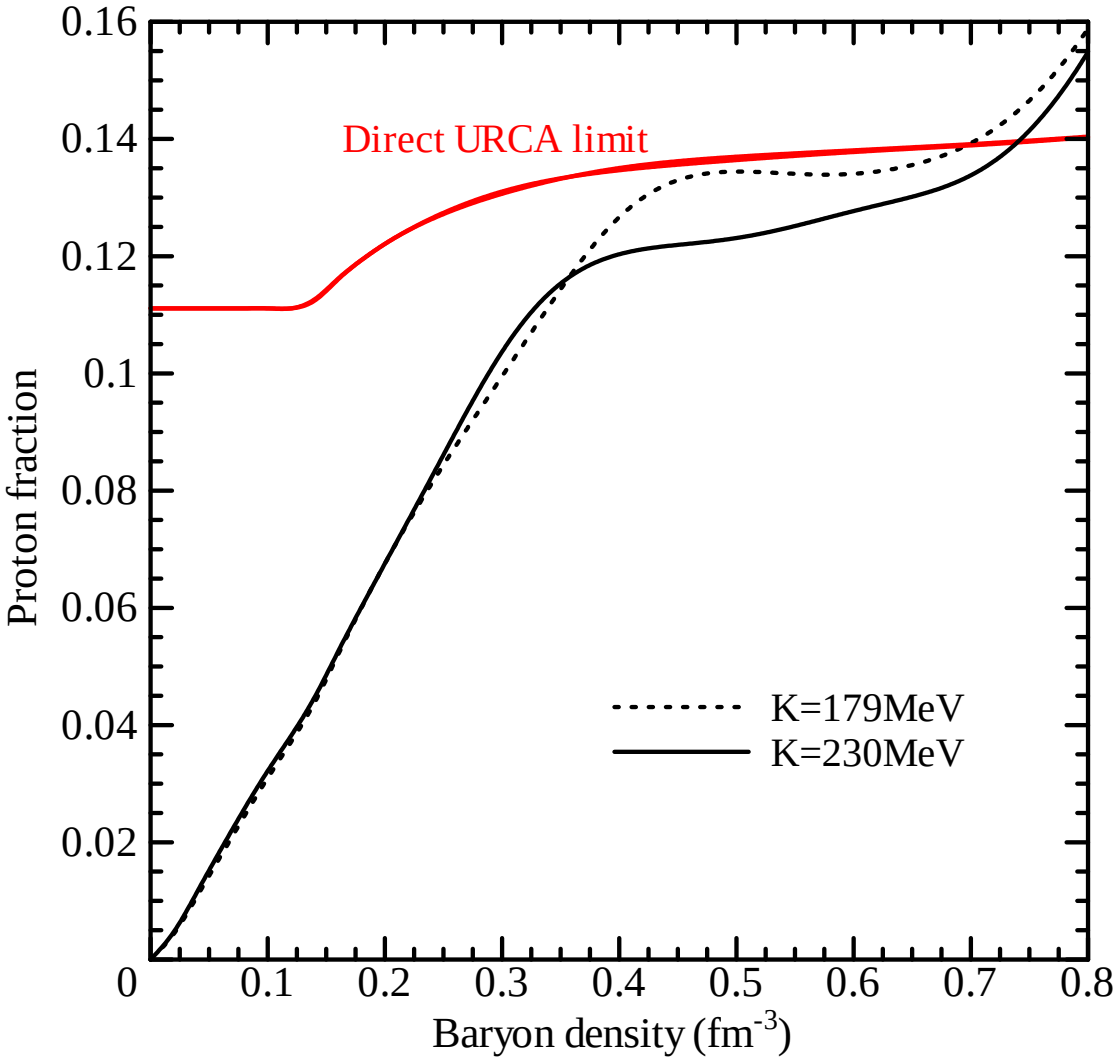

Figure 3: The black dashed and solid curves are proton fractions in the core of NS using the EOSs of $K_0 = 179$MeV and 230MeV, respectively. If the fraction exceeds the red curve from Eq. (48), the direct URCA cooling is possible in NSs.